Supplementary Information

Magnetic field-induced surface reconstruction of Fe-CoP nanostructures for enhanced oxygen evolution catalytic performance

JianLong Jiao [a,1], Jin-Hua Liu [a,1], WenYue Wang [a], LingYun Li [a], Ru Li [b], Shuai-Jie Wang [a], WenPeng Han [a,*], Yun-Ze Long [a,*], Seeram Ramakrishna [c]

[a] *Shandong Key Laboratory of Low Dimensional Materials and Polymer Composites, Qingdao University, Qingdao 266071, PR China*

[b] *Instrumental Analysis Center of Qingdao University, Qingdao 2266071, China*

[c] *Center for Nanotechnology & Sustainability, Department of Mechanical Engineering, College of Design and Engineering, National University of Singapore, 9 Engineering Drive 1, Singapore 117576*

[*] Corresponding authors.

E-mail addresses: yunze.long@qdu.edu.cn (Y.Z. Long) and han_wenpeng@163.com (W.P. Han).

[1] These two authors contributed equally to this work.

The file includes:

Section 1. Experimental Section

Section 2. Figures and Tables

magnetic field of 600 mT was applied during the preparation process; (b) Fe-CoP-600/800 mT indicates that a magnetic field of 800 mT was applied during the OER test for Fe-CoP-600.

Fig. S14. (a) Hydrogen evolution LSV curve (b) AC impedance diagram (c) Tafel plot (d) Fitted curve of C_{dl}.

Fig. S15. Cyclic voltammetry (CV) curves of different materials for HER: (a) Fe-CoP-600 indicates that a magnetic field of 600 mT was applied during the preparation process; (b) Fe-CoP-600/800 mT indicates that a magnetic field of 800 mT was applied during the OER test for Fe-CoP-600.

Figure S16. Different magnetic field directions relative to the catalyst : (a) LSV curve for oxygen evolution; (b) AC impedance plot; (c) Fitting curve of Cdl; (d-h) CV curves of OER (0°, 45°, 90°, 135°, and 180° relative to the catalyst surface).

Fig. S17. (a-e) Repeatability verification of the HER performance of Fe-CoP prepared under different magnetic fields (0, 200, 400, 600 and 800 mT).

Fig. S18. (a-e) Repeatability verification of EIS of HER prepared by Fe-CoP under different magnetic fields (0, 200, 400, 600 and 800 mT).

Fig. S19. (a-e) Verification of the repeatability of the Cdl of HER of Fe-CoP prepared under different magnetic fields (0, 200, 400, 600 and 800 mT).

Fig. S20. (a-e) Repeatability verification of the properties of Fe-CoP electrocatalysts prepared under different magnetic fields (0, 200, 400, 600 and 800 mT) and magnetic field-assisted enhancement.

Fig. S21. (a-e) Repeatability verification of EIS of Fe-CoP electrocatalysts under different magnetic fields (0, 200, 400, 600 and 800 mT) and magnetic field-assisted enhancement conditions.

Fig. S22. (a-e) Repeatability verification of Cdl of Fe-CoP electrocatalysts under different magnetic fields (0, 200, 400, 600 and 800 mT) and magnetic field-assisted enhancement conditions.

Figure S23. (a) TEM morphology of Fe-CoP-600 (b) XRD pattern of Fe-CoP-600

Figure S24. (a) Normalized LSV curve of OER (b) Normalized LSV curve of HER (c)

Section 1. Experimental Section

1.1. Chemicals.

Carbon paper (CP) was purchased from the Toray. Cobalt(II) chloride hexahydrate ($CoCl_2 \cdot 6H_2O$), ammonium chloride (NH_4Cl), and potassium hydroxide (KOH) were purchased from the Aladdin. Ferric chloride hexahydrate ($FeCl_3 \cdot 6H_2O$) was purchased from the Shanghai Gade Chemical Reagent. Sodium hypophosphite ($NaH_2PO_2 \cdot 2H_2O$) was purchased from the Ron. Deionized water (H_2O) was purchased from the Qingdao Chengda Distilled Water Co., Ltd. Anhydrous ethanol (C_2H_6O) was purchased from the National Pharmaceutical Chemical Reagents. All the reagents were used directly after purchase with any further processing.

1.2. Synthesis of Fe-CoP

Amorphous CoP/CP and Fe-CoP/CP were synthesized on carbon paper in one step by electrodeposition. Specifically, 2 mmol of cobalt(II) chloride hexahydrate, 2 mmol of iron(III) chloride hexahydrate, 5 mmol of ammonium chloride, and 5 mmol of sodium hypophosphite were dissolved in 50 mL of deionized water and stirred continuously until uniform to form the electro-deposition solution. A 1×1.5 cm^2 carbon paper was repeatedly washed with dilute hydrochloric acid, ethanol, and deionized water, and then dried in a vacuum drying oven as the catalyst carrier. Under different magnetic fields (0 mT, 200 mT, 400 mT and 600 mT), the treated carbon paper was used as the working electrode, the mercury-mercury oxide electrode as the reference electrode, and the carbon rod as the counter electrode. The electrochemical workstation was set to an input potential of -1 V and run for 30 min. After electro-deposition, the samples were repeatedly rinsed with anhydrous ethanol and deionized water and then dried in a vacuum drying oven.

1.3. Material Characterizations

This study analyzed the influence of magnetic field on the structure and performance of Fe-CoP-600 (600 indicates the magnetic field strength of 600 mT applied during the magnetic field-assisted deposition process) through a multi-scale

characterization system. The morphology and structure of the samples with and without applied magnetic field before and after oxygen evolution reaction (OER) tests were characterized by scanning electron microscopy (SEM, Phenom Pro, FEI Company) and transmission electron microscopy (TEM, FEI Tecnai G2 F20), and the elemental distribution was determined by SEM mapping. The surface composition and chemical state were analyzed by X-ray photoelectron spectroscopy (XPS) equipped with an Al Kα radiation source (Thermo Fisher Scientific Nexsa G2), and the binding energy was calibrated by the C 1s peak (284.8 eV). The X-ray diffraction (XRD) patterns of the obtained samples were tested by a Rigaku Ultima IV X-ray diffractometer. The magnetic characterization of the samples, including M-H and M-T curves, was tested using a Physical Property Measurement System (PPMS, EverCool II, Quantum Design, USA). All magnetic field-related operations in the experiment were supplied with magnetic fields by a magnetic field generator (wDs50, Tianrui Company, Shanghai).

1.4. Electrochemical Measurements

The electrochemical performance of the catalyst was tested on an electrochemical workstation (Kethon-CS301X), with a standard three-electrode system composed of a mercury oxide electrode, a graphite counter electrode, and the catalyst prepared in this work. The potential measured against the Hg/HgO electrode was converted to the potential against the reversible hydrogen electrode (RHE) according to the formula $E(RHE) = E(Hg/HgO) + 0.059 \times pH + 0.098$. Linear sweep voltammetry (LSV) curves were collected in 1.0 M KOH electrolyte at a scan rate of 5 mV/s. The LSV curves were corrected for IR and manually compensated by 90%, and the Tafel slope was calculated from the LSV curves. The double-layer capacitance was measured at scan rates of 100, 80, 60, 40, and 20 mV s^{-1}. The charge transfer resistance was determined by electrochemical impedance spectroscopy (EIS) in the frequency range of 0.1 to 10^5 Hz. The stability test was conducted by chronopotentiometry. All electrochemical measurements were performed at least three times to ensure data reliability and reproducibility.

Section 2. Figures and Tables

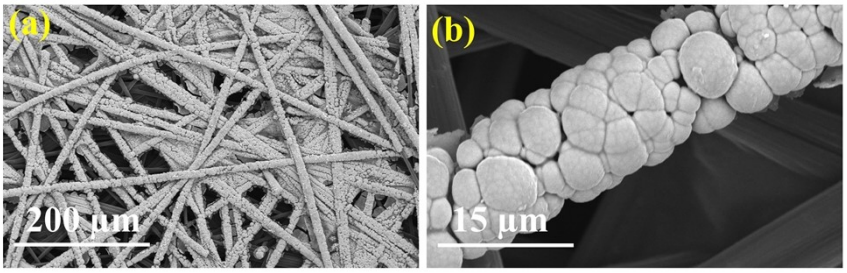

Fig. S1. (a-b) SEM images of Fe-CoP/CP

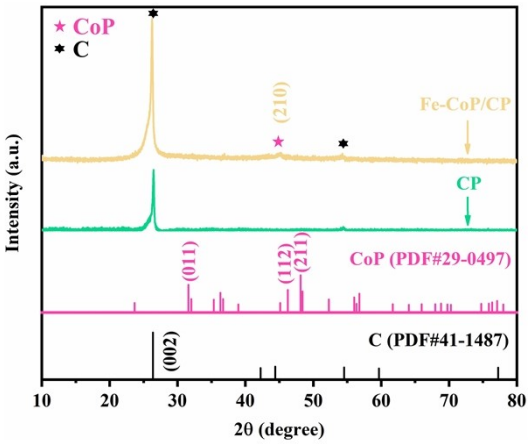

Fig. S2. The XRD patterns of CP and Fe-CoP/CP

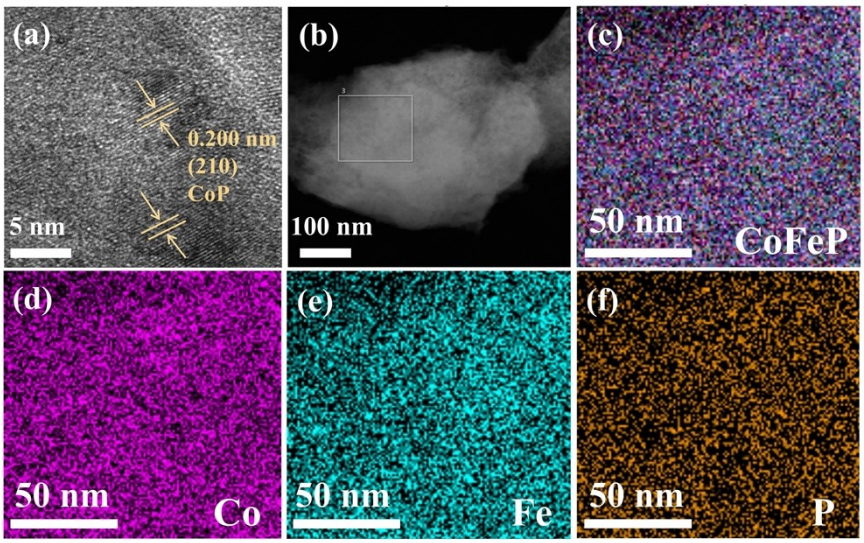

Fig. S3. (a) HRTEM images and **(b-f)** EDX mapping images of Fe-CoP/CP

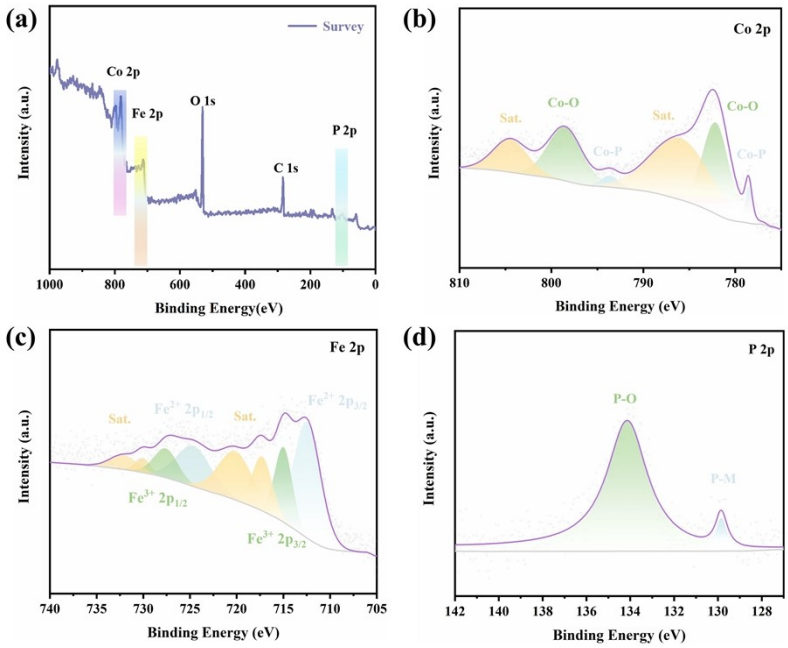

Fig. S4. XPS spectra of Fe-CoP/CP: **(a)** Survey **(b)** Co 2p **(c)** Fe 2p **(d)** P 2p

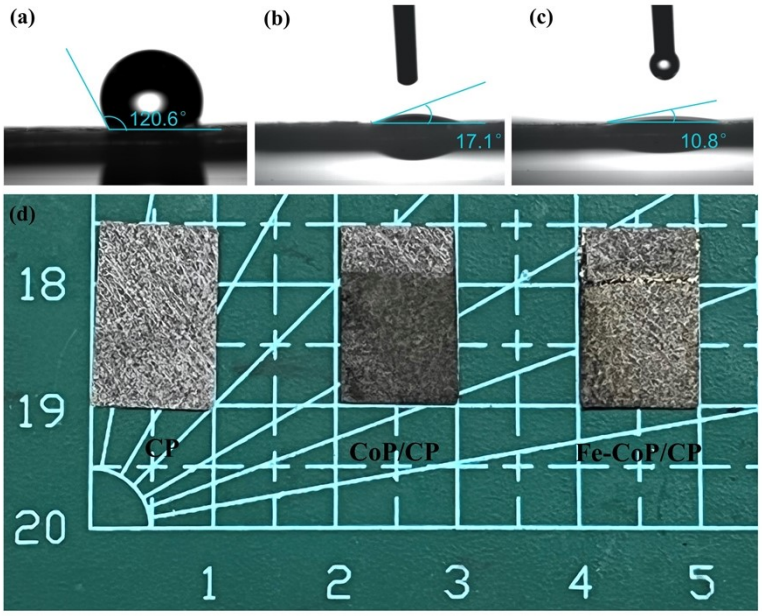

Fig. S5. Water contact angles: **(a)** CP **(b)** CoP/CP **(c)** Fe-CoP/CP **(d)** optical photos of the materials

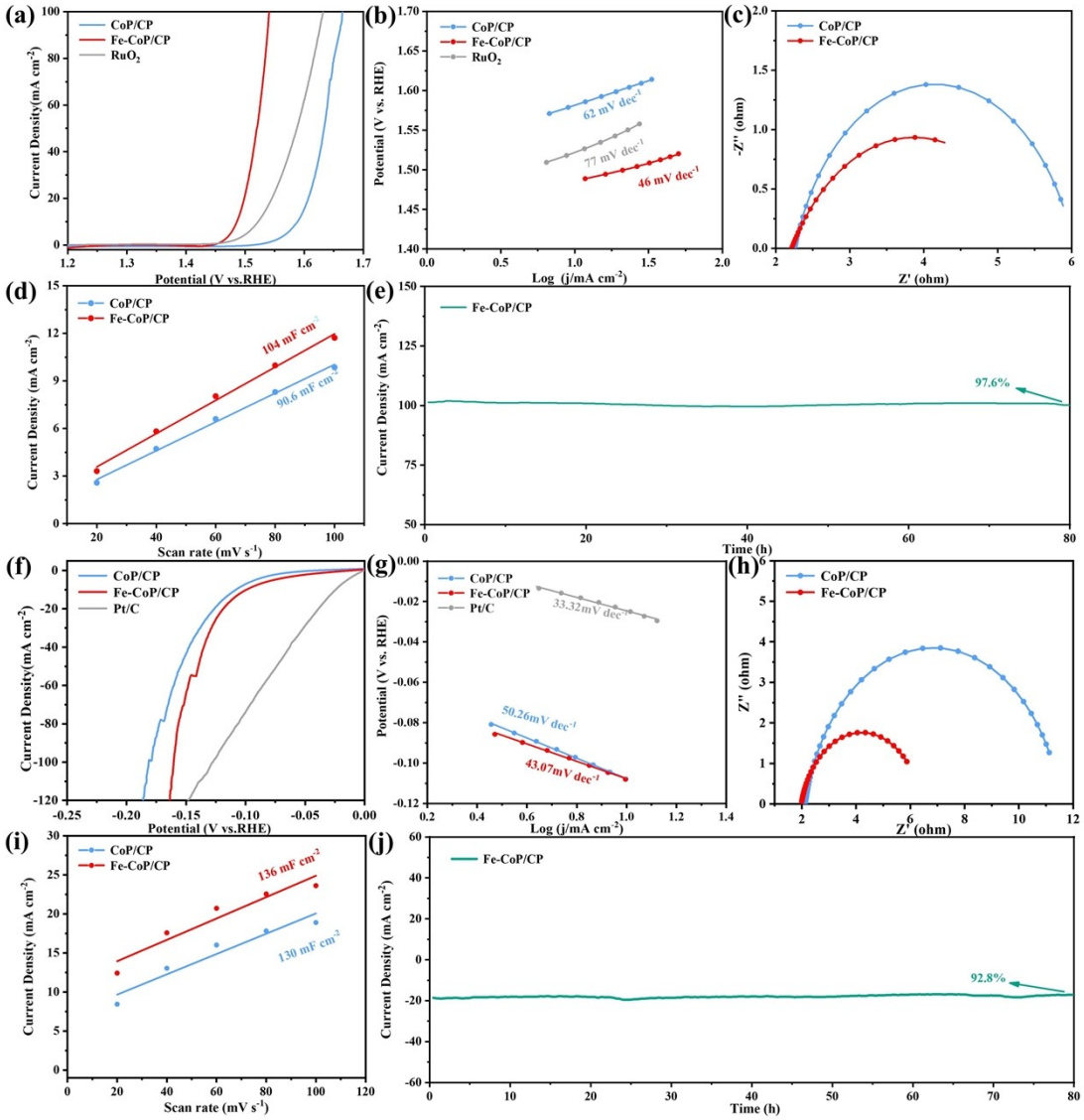

Fig. S6. Oxygen evolution from Fe-CoP/CP: **(a)** LSV curve **(b)** Tafel plot **(c)** AC impedance diagram **(d)** fitted C_{dl} curve **(e)** OER stability test

Hydrogen evolution from Fe-CoP/CP: **(f)** LSV curve **(g)** Tafel plot **(h)** AC impedance diagram **(i)** fitted C_{dl} curve **(j)** HER stability test

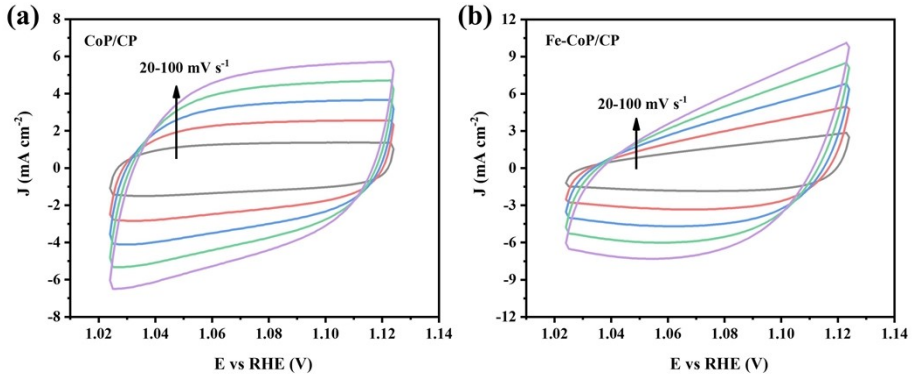

Fig. S7. CV curves of OER for different materials: **(a)** CoP/CP **(b)** Fe-CoP/CP

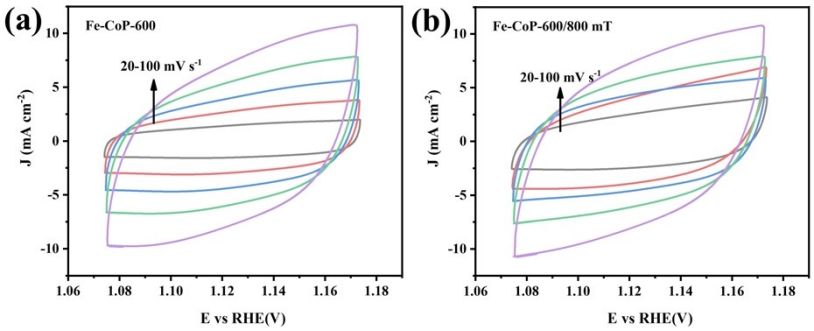

Fig. S8. Cyclic voltammetry (CV) curves of HER for different materials: **(a)** CoP/CP **(b)** Fe-CoP/CP

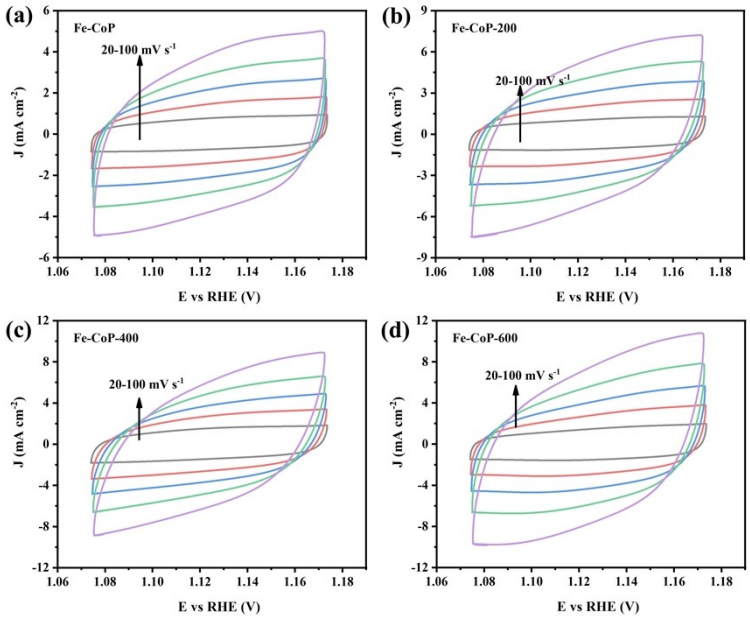

Fig. S9. CV curves of OER of Fe-CoP prepared under different magnetic fields: (a) 0 mT (b) 200 mT (c) 400 mT (d) 600 mT (e) 800 mT.

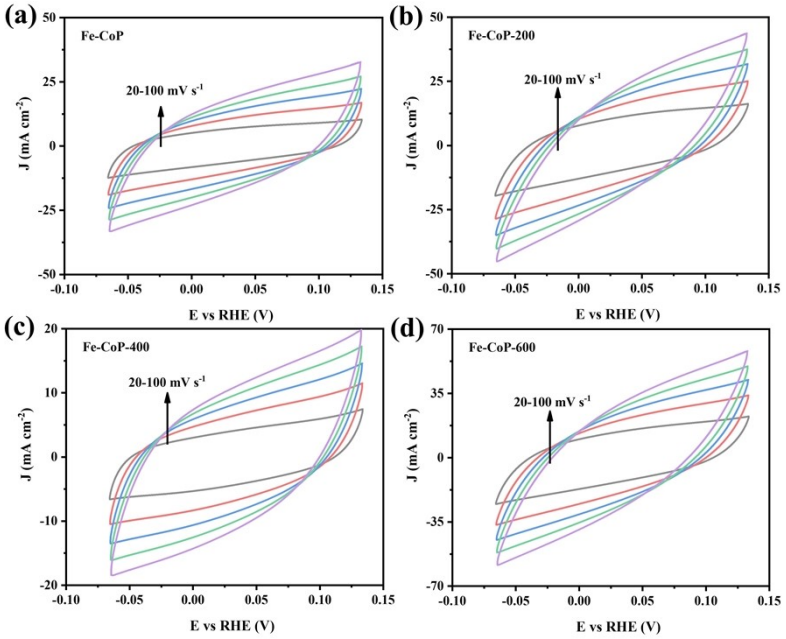

Fig. S10. CV curves of hydrogen evolution for Fe-CoP prepared under different magnetic fields: (a) 0 mT (b) 200 mT (c) 400 mT (d) 600 mT (e) 800 mT.

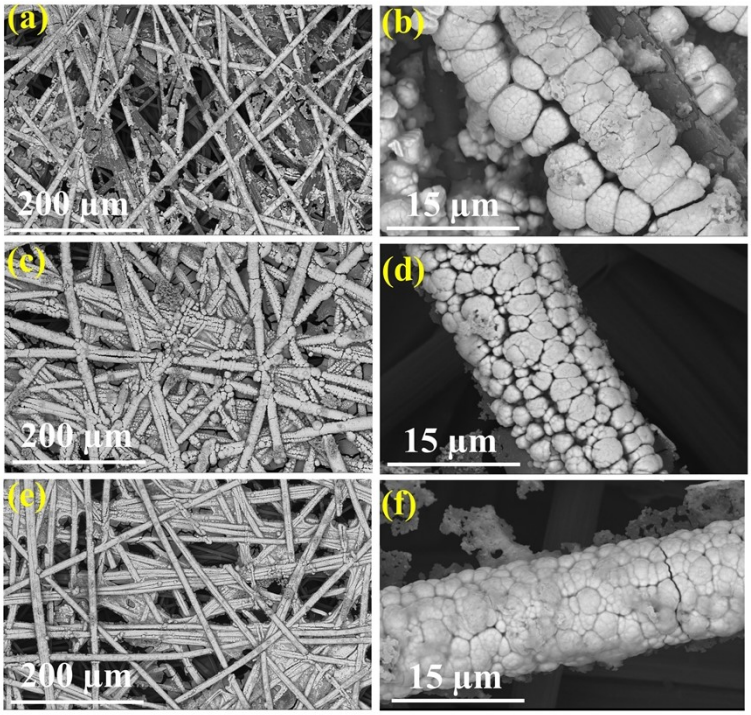

Fig. S11. SEM images of Fe-CoP/CP-600: **(a-b)** deposition time 5 min, **(c-d)** deposition time 10 min, **(e-f)** deposition time 20 min

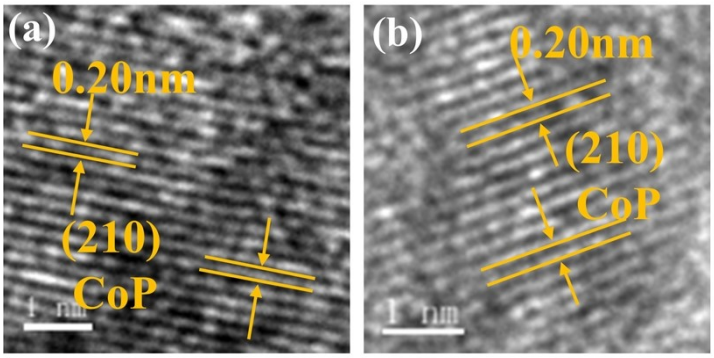

Fig. S12. TEM images of Fe-CoP/CP-600

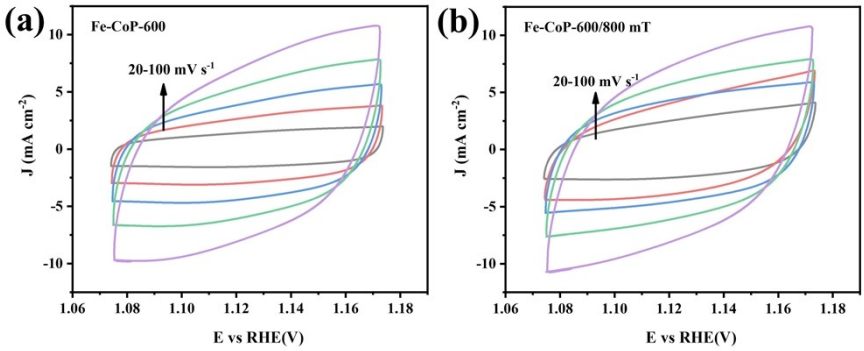

Fig. S13. CV curves of OER for different materials:

(a) Fe-CoP-600 indicates that a magnetic field of 600 mT was applied during the preparation process.

(b) Fe-CoP-600/800 mT indicates that a magnetic field of 800 mT was applied during the OER test for Fe-CoP-600.

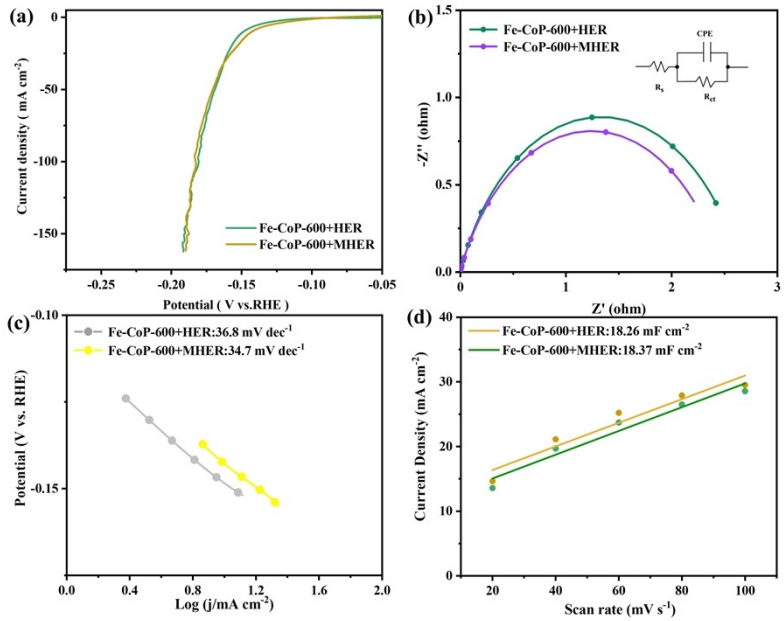

Fig. S14. (a) Hydrogen evolution LSV curve **(b)** AC impedance diagram **(c)** Tafel plot **(d)** Fitted curve of C_{dl}

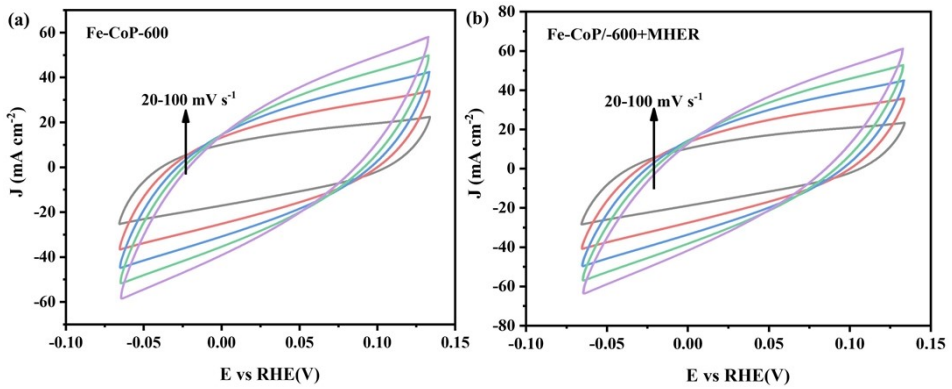

Fig. S15. CV curves of HER for different materials:

(a) Fe-CoP-600 indicates that a magnetic field of 600 mT was applied during the preparation process.

(b) Fe-CoP-600/800 mT indicates that a magnetic field of 800 mT was applied during the OER test for Fe-CoP-600.

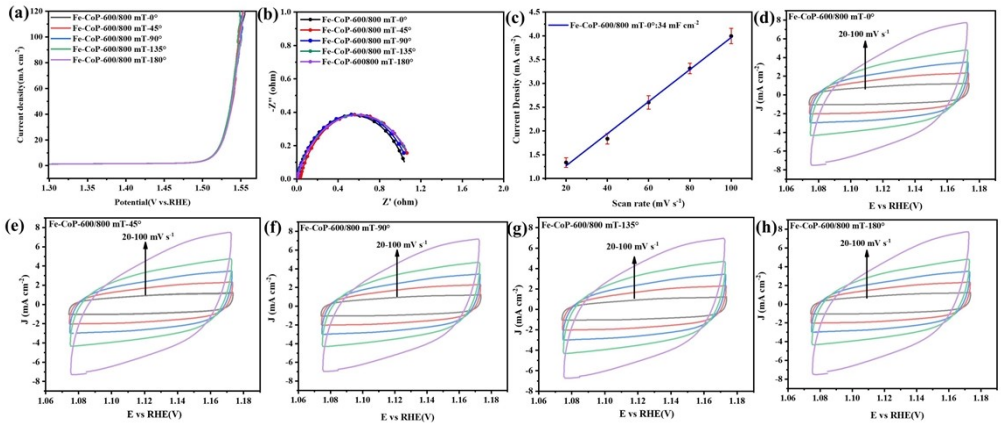

Figure S16. Different magnetic field directions relative to the catalyst :

(a) LSV curve for oxygen evolution. **(b)** AC impedance plot. **(c)** Fitting curve of C_{dl}.

(d-h) CV curves of OER(0°, 45°, 90°, 135°, and 180° relative to the catalyst surface).

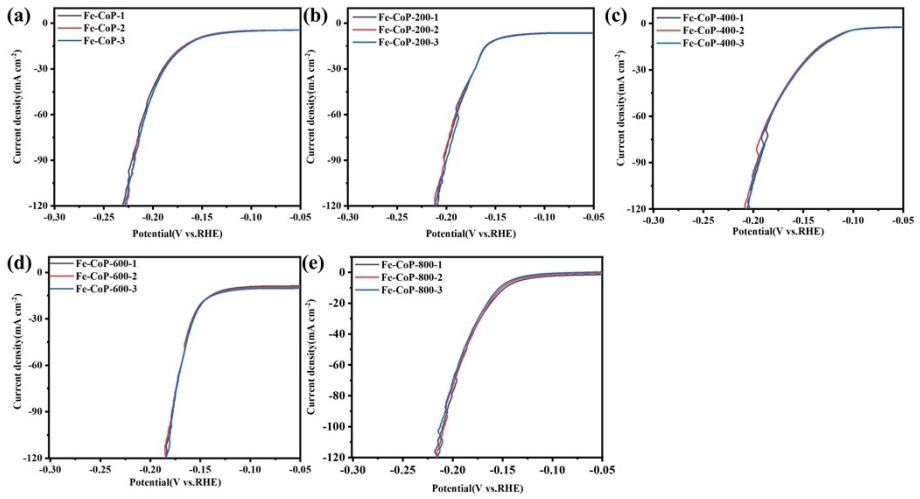

Figure S17. (a-e) Repeatability verification of the HER performance of Fe-CoP prepared under different magnetic fields (0,200,400,600 and 800 mT)

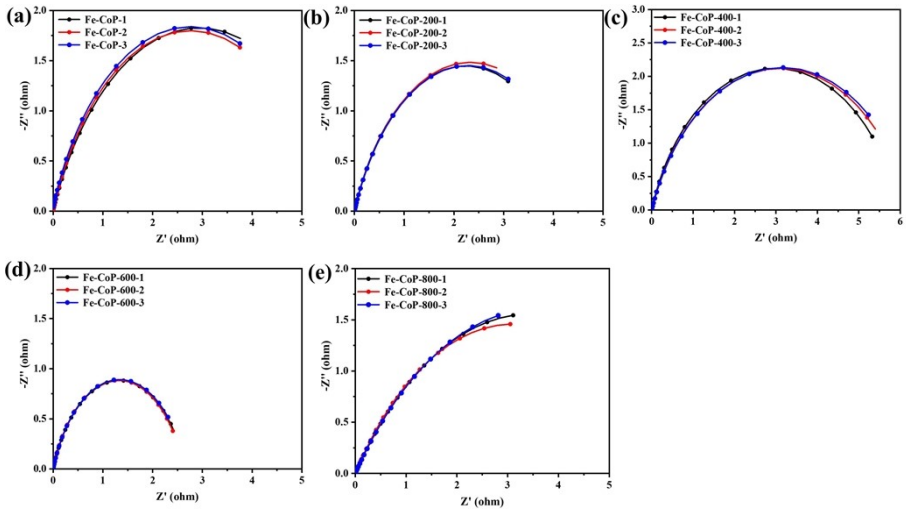

Figure S18. (a-e) Repeatability verification of EIS of HER prepared by Fe-CoP under different magnetic fields (0,200,400,600 and 800 mT)

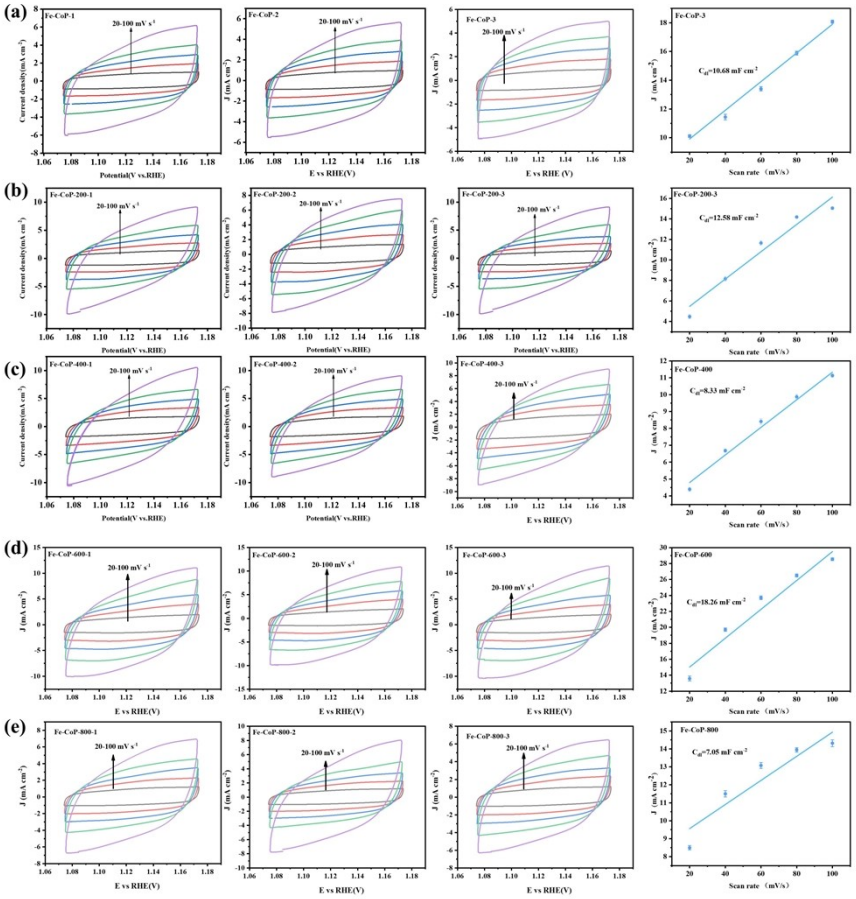

Figure S19. (a-e) Verification of the repeatability of the Cdl of HER of Fe-CoP prepared under different magnetic fields(0,200,400,600 and 800 mT)

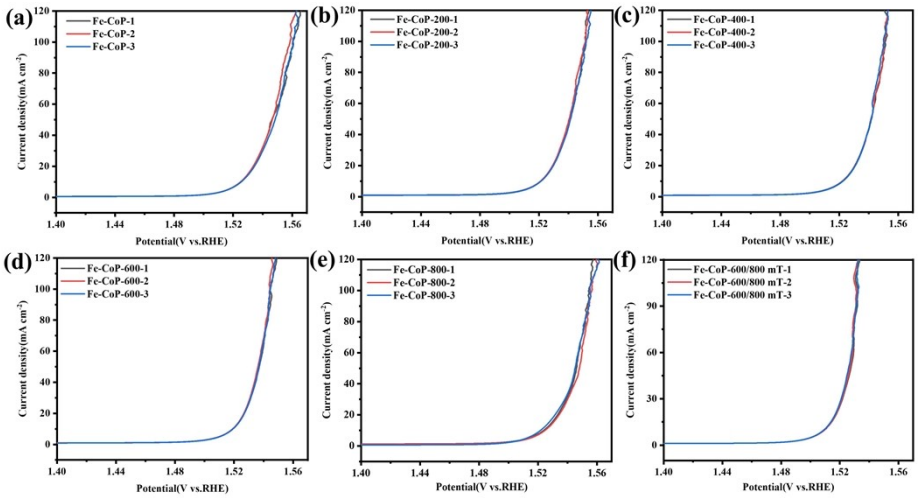

Figure S20. (a-e) Repeatability Verification of the Properties of Fe-CoP Electrocatalysts Prepared under Different Magnetic Fields(0,200,400,600 and 800 mT) and Magnetic Field-Assisted Enhancement

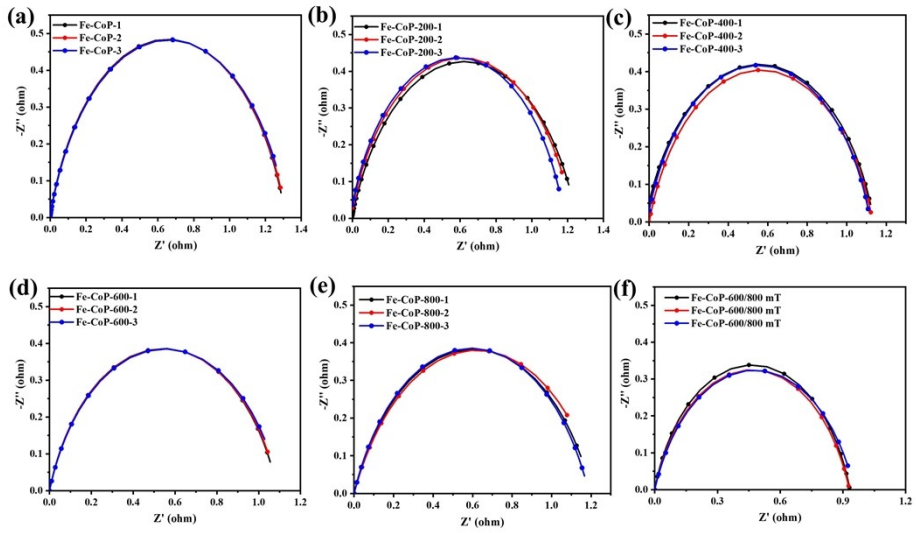

Figure S21. (a-e) Repeatability verification of EIS of Fe-CoP electrocatalysts under different magnetic fields (0,200,400,600 and 800 mT) and magnetic field-assisted enhancement conditions

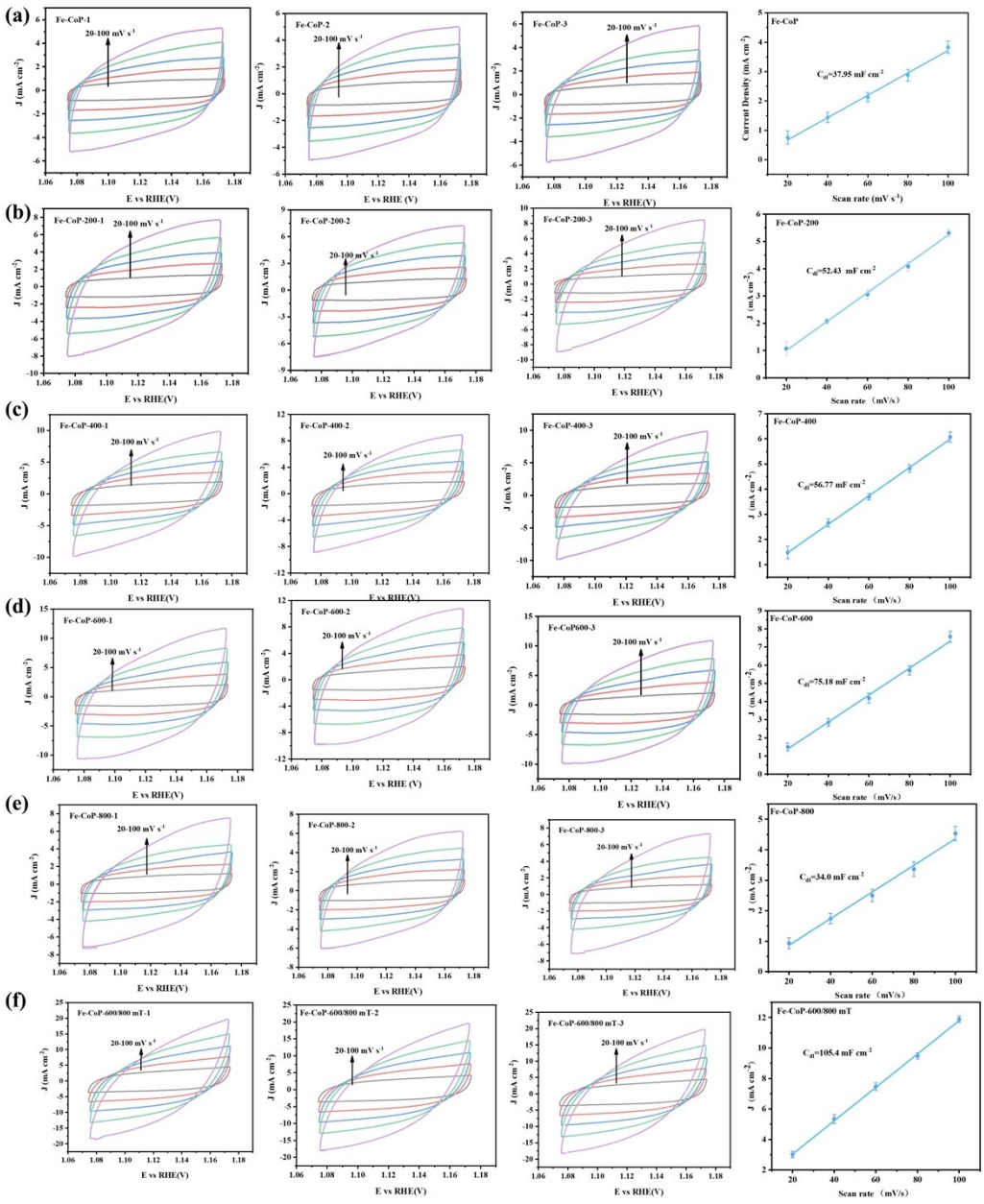

Figure S22. (a-e) Repeatability verification of Cdl of Fe-CoP electrocatalysts under different magnetic fields (0,200,400,600 and 800 mT) and magnetic field-assisted enhancement conditions

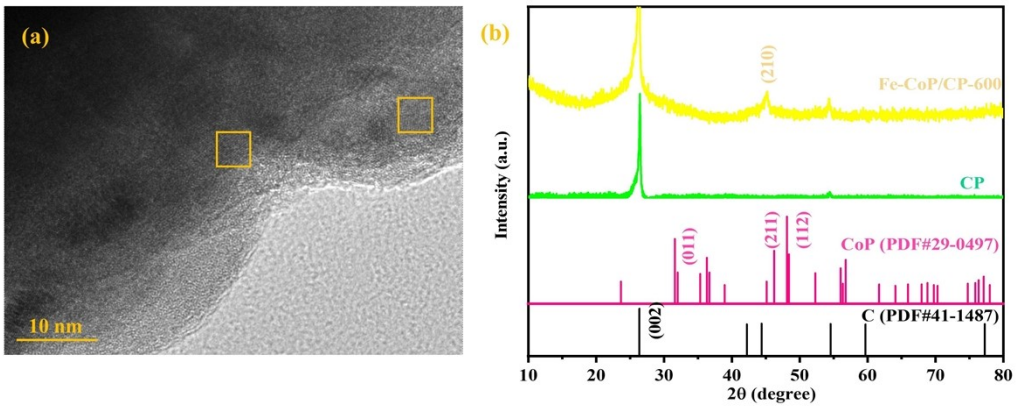

Figure S23. (a) TEM morphology of Fe-CoP-600 (b) XRD pattern of Fe-CoP-600

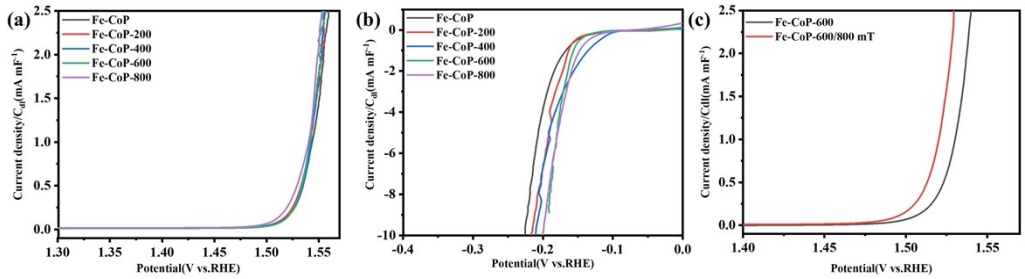

Figure S24. (a) Normalized LSV curve of OER (b) Normalized LSV curve of HER (c) Normalized LSV curve of OER for Fe-CoP-600 samples under different magnetic fields (0 mT, 800 mT)

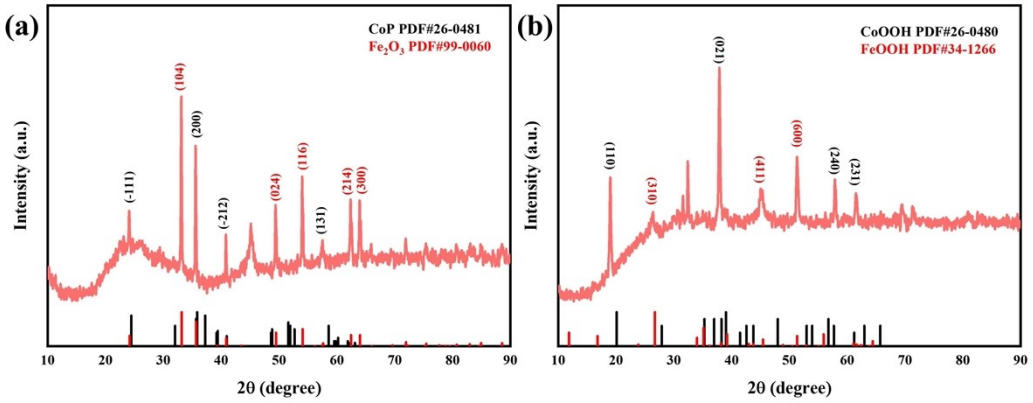

Figure S25. XRD patterns of Fe-CoP-600 after OER tests with and without magnetic field.

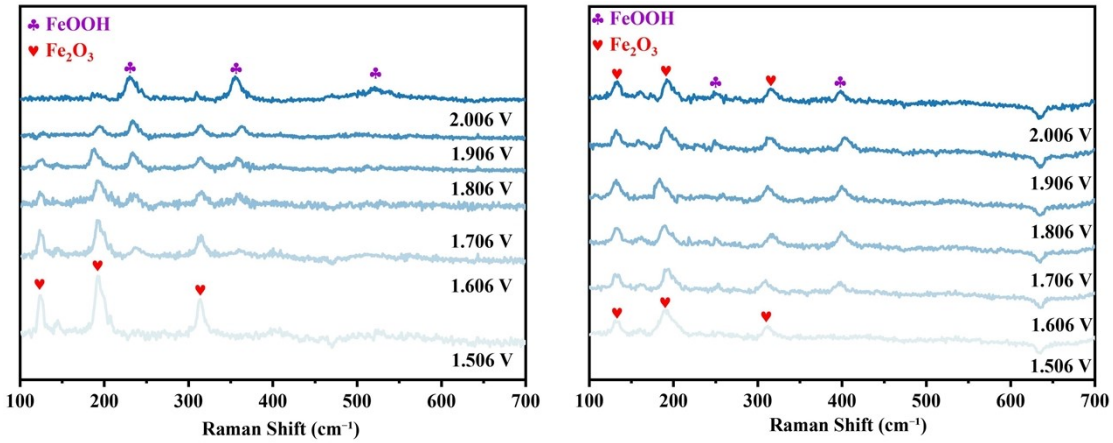

Figure S26. (a) In-situ Raman spectra of the catalyst at different OER voltages without an external magnetic field. (b) In-situ Raman spectra of the catalyst at different OER voltages with an external magnetic field.

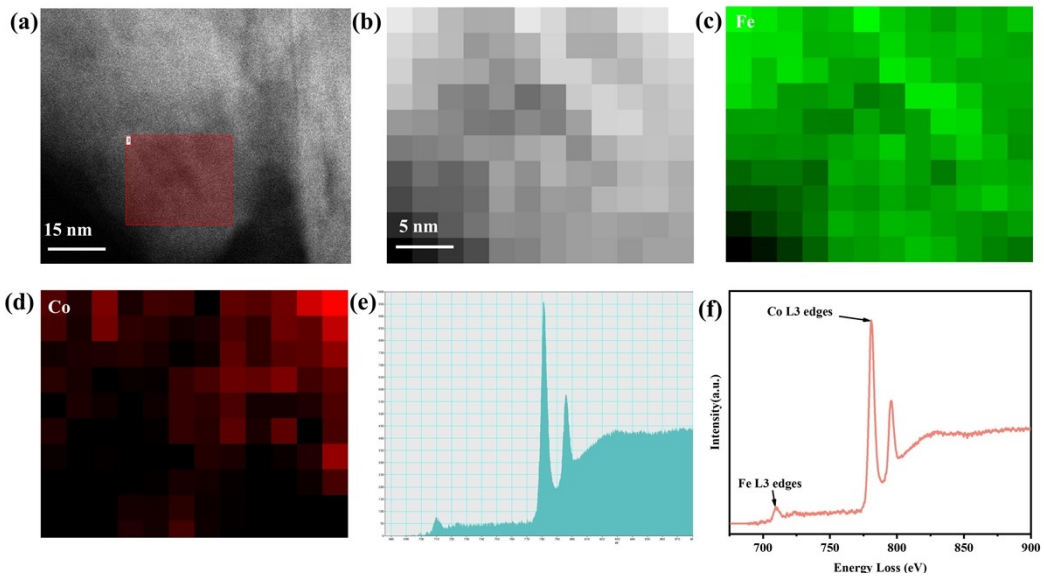

Figure S27. (a) STEM image of the sample. (b) Enlarged STEM image of the red-boxed area in (a). (c) EELS mapping of Fe. (d) EELS mapping of Co. (e) Spatial mapping of EELS spectra. (f) EELS spectrum of area (b), showing Fe/Co L_3/L_2 edges.

Table S1. Comparisons of Fe-CoP-600/800 mT with other reported catalysts for OER performance.

Catalysts	Electrolyte Solution	OER@10 mA cm $^{-2}$	Magnetic field	Ref
Fe_2P	1 M KOH	508 mV	1000 mT	1
CFO@CoBDC/MCV	1M KOH	304 mV	600 mT	2
NiCoFe/MOF-74	1M KOH	214 mV	AC-5.184 mT	3
$NiCo_{2-x}Fe_xO_4$	1M KOH	202mV	500 mT	4
NiFe/NiFeOOH core/shell NPs	1M KOH	209.2 mV	AC-3.9 mT	5
(Ru-Ni)O_x@NF	1M KOH	286mV	400 mT	6
$Co_{3-x}Fe_xO_4$	1M KOH	350mV	500 mT	7
Fe-CoP-600	1M KOH	300 mV	800 mT	**This work**

Table S2. COMSOL Multiphysics simulation parameters for magnetic field-assisted ion deposition.

Parameter	Value/Setting
Software	COMSOL Multiphysics 6.2
Physics modules	Electrostatics (es) + Particle Tracing for Fluid Flow (fpt)
Geometry dimension	3D
Simulation domain	5 μm × 5 μm × 40 μm (cylinder)
Carbon fiber diameter	1.6 μm
Co^{2+} concentration	40 mM (2 mmol in 50 mL)
Fe^{3+} concentration	40 mM (2 mmol in 50 mL)
Magnetic field strength (B_0)	0, 200, 400, 600, 800, 1000 mT (parametric sweep)
Magnetic field direction	Uniform, perpendicular to electrode surface (z-axis)
Magnetic field gradient	None (uniform field assumed)
Applied potential (V_0)	-1 V

Parameter	Value/Setting
Temperature	298 K (room temperature)
Electrolyte relative permittivity	78 (water)
Boundary condition (electrode)	Electric potential: V_0 = -1 V; Wall (Freeze): particles stick upon contact
Boundary condition (outer)	Zero charge ($n \cdot D = 0$)
Number of particles per release	500 (Co^{2+}) + 500 (Fe^{3+})
Force model	Electric force ($F = qE$) + Lorentz force ($F = qv \times B$)
Mesh type	Free tetrahedral; refined near fiber (min: 0.03 μm, max: 0.7 μm)
Solver	Stationary (electrostatics) + Time-dependent (particle tracing)

Reference

1. F. Chen, C. Shen, Y. Zhu, Y. Liu, D. Zhou, L. Huang, L. Shi, H. Zhang, S. Cao and R. Jia, *Applied Surface Science*, 2024, **653**, 159357.
2. S. Ma, K. Wang, M. Rafique, J. Han, Q. Fu, S. Jiang, X. Wang, T. Yao, P. Xu and B. Song, *Angew Chem Int Ed Engl*, 2024, **63**, e202412821.
3. H.-b. Zheng, Y.-l. Wang, P. Zhang, F. Ma, P.-z. Gao, W.-m. Guo, H. Qin, X.-p. Liu and H.-n. Xiao, *Chemical Engineering Journal*, 2021, **426**, 130785.
4. L.-L. Hao, J.-Y. Hu, J. Li, Y.-J. Gao, Y.-S. Meng and T. Liu, *ACS Catalysis*, 2025, **15**, 5640-5650.
5. D. Peng, C. Hu, X. Luo, J. Huang, Y. Ding, W. Zhou, H. Zhou, Y. Yang, T. Yu, W. Lei and C. Yuan, *Small*, 2023, **19**, e2205665.
6. H. Li, Q. Quan, H. Dong, Y. Zhang, P. Xie, D. Chen, D. Yin, C. Y. Wong and J. C. Ho, *Advanced Functional Materials*, 2025, **35**, 2420810.
7. T. Wu, X. Ren, Y. Sun, S. Sun, G. Xian, G. G. Scherer, A. C. Fisher, D. Mandler, J. W. Ager, A. Grimaud, J. Wang, C. Shen, H. Yang, J. Gracia, H. J. Gao and Z. J. Xu, *Nat Commun*, 2021, **12**, 3634.